Large Molecule Therapeutics

Molecular Cancer Therapeutics

Novel Neutralizing Hedgehog Antibody MEDI-5304 Exhibits Antitumor Activity by Inhibiting Paracrine Hedgehog Signaling

Neil R. Michaud[1], Youzhen Wang[1], Kristen A. McEachern[1], Jerold J. Jordan[1], Anne Marie Mazzola[1], Axel Hernandez[1], Sanjoo Jalla[2], Jon W. Chesebrough[2], Mark J. Hynes[3], Matthew A. Belmonte[1], Lidong Wang[3], Jaspal S. Kang[4], Jelena Jovanović[5], Naomi Laing[1], David W. Jenkins[1], Elaine Hurt[2], Meina Liang[7], Christopher Frantz[8], Robert E. Hollingsworth[2], Diane M. Simeone[3], David C. Blakey[6], and Vahe Bedian[1]

Abstract

The hedgehog pathway has been implicated in the tumorigenesis, tumor progression, and metastasis of numerous human cancers. We generated the first fully human hedgehog antibody MEDI-5304 and characterized its antitumor activity and preclinical toxicology. MEDI-5304 bound sonic hedgehog (SHH) and Indian hedgehog (IHH) with low picomolar affinity and neutralized SHH and IHH activity in cellular mGLI1 reporter assays. The antibody inhibited transcription of hedgehog target genes and osteoblast differentiation of C3H10T1/2 cells. We evaluated the activity of MEDI-5304 *in vivo* in model systems that allowed us to evaluate two primary hypotheses of hedgehog function in human cancer, paracrine signaling between tumor and stromal cells and cancer stem cell (CSC) self-renewal. MEDI-5304 displayed robust pharmacodynamic effects in stromal cells that translated to antitumor efficacy as a single agent in an HT-29/MEF coimplantation model of paracrine hedgehog signaling. MEDI-5304 also improved responses to carboplatin in the HT-29/MEF model. The antibody, however, had no effect as a single agent or in combination with gemcitabine on the CSC frequency or growth of several primary pancreatic cancer explant models. These findings support the conclusion that hedgehog contributes to tumor biology via paracrine tumor-stromal signaling but not via CSC maintenance or propagation. Finally, the only safety study finding associated with MEDI-5304 was ondontodysplasia in rats. Thus, MEDI-5304 represents a potent dual hedgehog inhibitor suitable for continued development to evaluate efficacy and safety in human patients with tumors harboring elevated levels of SHH or IHH. *Mol Cancer Ther; 13(2); 386–98. ©2013 AACR.*

Introduction

Hedgehog was identified in *Drosophila* as a mediator of embryonic patterning. There are three members of the hedgehog family in mammals, sonic hedgehog (SHH), Indian hedgehog (IHH), and desert hedgehog (DHH), which specify tissue patterning and regulate organ homeostasis by affecting cell growth and differentiation (1, 2). The hedgehog proteins are ligands for the 12-pass membrane spanning receptor Patched (PTCH), which normally represses the function of the G protein-coupled receptor (GPCR)-like transmembrane protein Smoothened (SMO; ref. 3). Upon binding by hedgehog ligands, repression of SMO by PTCH is relieved, allowing SMO to signal through members of the Gli family of transcription factors. Activation of transcription leads to the synthesis of pathway components such as GLI1 and PTCH1, which in turn drives cell proliferation and survival.

Dysregulation of the hedgehog/SMO pathway is implicated in tumorigenesis. Mutations that inactivate PTCH or constitutively activate SMO have been described in basal cell carcinoma (BCC), medulloblastoma, and rhabomyosarcoma (4). Overexpression of SHH or IHH has been described in numerous tumor types (5–9), and concomitant upregulation of GLI1 and PTCH1 has been observed (9–11). Ectopic overexpression of SHH in preclinical models can induce tumor formation, including BCCs and pancreatic neoplasia (11, 12), supporting the view that

Authors' Affiliations: [1]Oncology iMED, AstraZeneca-R&D Boston, Waltham, Massachusetts; [2]Oncology Research, MedImmune LLC, Gaithersburg, Maryland; [3]Translational Oncology Program, University of Michigan, Ann Arbor, Michigan; [4]Amgen British Columbia, Burnaby, British Columbia, Canada; [5]Lead Generation-Research, MedImmune LLC, Granta Park, Cambridge, United Kingdom; [6]Oncology iMED, AstraZeneca, Alderley Park, Macclesfield, United Kingdom; [7]Clinical Pharmacology and DMPK, MedImmune LLC, Hayward, California; and [8]Biologics Safety Assessment, MedImmune LLC, Mountain View, California

Note: Supplementary data for this article are available at Molecular Cancer Therapeutics Online (http://mct.aacrjournals.org/).

Current address for J.S. Kang: Innovative Targeting Solutions Inc., Burnaby, British Columbia, Canada.

Corresponding Authors: Neil R. Michaud, 28 Bouffard Drive, Marlborough, MA 01752. E-mail: nrmichaud706@gmail.com; and Vahe Bedian, Oncology iMED, AstraZeneca-R&D Boston, 35 Gatehouse Drive, Waltham, MA 02451. Phone: 781-839-4613; E-mail: vahe.bedian@astrazeneca.com

doi: 10.1158/1535-7163.MCT-13-0420

pathway activation promotes tumorigenesis in a ligand-dependent manner.

Dependence of tumors on HH/SMO signaling for growth and metastasis has been demonstrated with various pathway inhibitors. The natural product cyclopamine and its derivative saridegib (IPI-926) are reported to directly antagonize SMO and inhibit the growth of numerous tumor cell lines *in vitro* and *in vivo* either alone or in combination with chemotherapy (13–16). However, a challenge with using cyclopamine-related molecules is the potential for off-target effects in tumor cells when used at elevated concentrations, confounding whether observed biologic effects can be attributed to inhibiting HH/SMO function. Yet, other more selective inhibitors have implicated hedgehog in tumor growth. The SMO antagonist vismodegib, structurally unrelated to cyclopamine, impaired the growth of a medulloblastoma tumor model driven by mutation of *PTCH1* and human xenograft tumors overexpressing SHH (8, 17). Vismodegib has shown clinical activity in patients with BCC and medulloblastoma and was recently approved for the treatment of metastatic and locally advanced BCC (18, 19). The mouse monoclonal antibody (mAb) 5E1 has been used extensively as a tool to probe hedgehog biology by specifically blocking ligand-dependent pathway activation (20). 5E1 neutralized the GLI1 reporter in cells, which correlated with inhibition of primary tumor cell proliferation *in vitro* (6, 10), and it attenuated the growth of colorectal tumor xenografts and basal-like mouse mammary tumors *in vivo* (8, 9).

Several models have been proposed to explain how overexpression of hedgehog ligands may lead to the development of cancer (4). In the first model, autocrine signaling stimulates tumor cell proliferation. In the second model, paracrine signaling by SHH secreted by tumor cells activates SMO signaling in stromal cells, which in turn results in the production of factors that enhance tumor cell growth. Finally, SHH function has been implicated in self-renewal of cancer stem cells (CSC) in various tumor types (21). As such, SHH may promote tumorigenesis or relapse following treatment with chemotherapy and/or radiation by driving CSC self-renewal and propagation.

We describe here the isolation of two human antibodies, 6D7 and 3H8, with high affinity but differential selectivity for hedgehog proteins. 6D7 neutralizes SHH and IHH signaling and biologic activity in osteoblasts, whereas 3H8 neutralizes only SHH activity. 6D7 was renamed MEDI-5304 and was used to evaluate the paracrine signaling and the CSC hypotheses, because it represents a potent and selective agent to probe hedgehog biology in preclinical models. MEDI-5304 demonstrated pharmacodynamic and corresponding antitumor activity in an *in vivo* tumor cell-mouse embryonic fibroblast (MEF; HT-29/MEF) coimplantation model of paracrine hedgehog signaling and combination efficacy with carboplatin. Yet, MEDI-5304 had no effect on CSCs in primary pancreatic tumor explant models *in vivo* or derived tumorspheres. Finally, there were no drug-related toxicities for MEDI-5304 in exploratory toxicology studies performed in rat and cynomolgus monkeys, except for mild ondontodysplasia of rat incisors, a finding that does not translate to humans. These findings suggest that targeting the hedgehog pathway with a neutralizing antibody represents a promising therapeutic approach for human cancers in which overexpression of hedgehog ligands plays a prominent role.

Materials and Methods

Cell lines and primary human samples

Colo205 and HT-29 tumor cell lines and the C3H10T1/2 mouse mesenchymal cell line were obtained from American Type Culture Collection (ATCC). These cell lines were cultured according to ATCC instructions and were tested and authenticated by the AstraZeneca cell bank using DNA fingerprinting short-tandem repeat (STR) assays. All revived cell lines were used within 20 passages for a period of less than 6 months. MEFs from C57BL/6 mice treated with mitomycin C were obtained from Global Stem. Pancreatic adenocarcinoma tissue samples were obtained from patients who underwent pancreatic resection at University of Michigan Medical Center (Ann Arbor, MI) from 2010 to 2011 by using the Institutional Review Board (IRB)–approved guidelines. The pancreatic tumor tissue was used to develop low-passage xenografts in nonobese diabetic/severe combined immunodeficient (NOD/SCID) mice as we have described previously (22).

In vitro hedgehog-binding ELISA

Microtiter plates coated with 200 ng of recombinant human SHH (hSHH) C24II or h/mIHH C28II (R&D Systems; #1845-SH-025/CF and 1705-HH/CF) in PBS and subsequently blocked with 1% bovine serum albumin (BSA; Sigma; #3156) in PBS for 1 hour at room temperature were incubated with serially diluted primary antibodies 6D7 and 3H8 in TBS+Tween 20 (TBS-T) for 16 hours on a shaker at 4°C. After washing in TBS-T, secondary goat anti-human immunoglobulin G (IgG) H+L antibody (KPL; #074-1006) diluted at 1:50,000 in TBS-T was incubated for 1 hour at room temperature. Relative light units (RLU) were determined in a Spectromax 5e luminometer after incubation (10 minutes) with peroxidase substrate (Sigma; #CPS-2-60).

Binding kinetics determined with surface plasmon resonance

Surface plasmon resonance (SPR) experiments were performed on a Biacore T100 biosensor (GE Healthcare) at 25°C. Of note, 150 resonance units (RU) of protein G′ (Sigma-Aldrich) were covalently immobilized on the surface of the C1 chip by using standard amine coupling chemistry, according to the manufacturer's instructions (BIAapplications Handbook; GE Healthcare). The same procedure was used to immobilize 150 RU of 5E1 mouse IgG1 directly on the C1 surface. The first flow cell was left empty and served as a reference surface following EDC/NHS activation and ethanolamine deactivation.

Low-density surfaces with ≤100 RU of each antibody were generated to minimize mass transport effects. Recombinant hedgehog proteins run in HBS-P buffer (10 mmol/L HEPES, 150 mmol/L NaCl, and 0.0005% surfactant P20; from GE Healthcare) supplemented with 200 μg/mL recombinant human albumin (Sigma) were used as analytes. A titration series of analyte was injected for 5 minutes at 50 μL/min followed by 15 minutes of dissociation. Interaction surfaces were regenerated with 10 mmol/L of glycine at pH 1.75.

Sensorgrams were analyzed by using the Biacore T100 evaluation software, version 2.0.1 (GE Healthcare). All sensorgrams were double referenced. The average response of all blank injections was subtracted from all sensorgrams to remove systematic artifacts in the experimental and reference flow cells. The kinetic parameters were derived by fitting the data with a simple 1:1 bimolecular binding model that included a term for mass transport.

NIH 3T3 mGLI1 reporter assay

NIH 3T3 cells engineered with a luciferase reporter driven by eight copies of the GLI1-binding site in the promoter were plated (75,000 cells/well) in media containing 0.5% FBS. Cells were treated with 1 μg/mL recombinant hSHH C24II or h/mIHH C28II alone or with serially diluted antibodies for 24 hours in media containing 0.5% FBS. RLUs were determined in a luminometer (Tecan Infinite M200) after 10 minutes of incubation at room temperature with firefly luciferase reagent (Promega).

Osteoblast differentiation assay

C3H10T1/2 cells were plated (5,000 cells/well in 96-well plates or 3,000 cells/well in 384-well plates). Recombinant hedgehog ligands were mixed with serially diluted hedgehog antibodies and incubated with cells for 72 hours. Cells were lysed in radioimmunoprecipitation assay (RIPA) cell lysis buffer (Thermol Scientific) and assayed for alkaline phosphatase activity by using the chromogenic substrate p-nitrophenylphosphate (Sigma) at 1 mg/mL, pH 9.8 and absorbance at 405 nm was measured.

Quantitative reverse transcription PCR

Quantitative reverse transcription PCR (qRT-PCR) was used to determine the target modulation in C3H10T1/2 cells, xenograft tumors, and skin samples. RNA was isolated from homogenized snap-frozen tumor or skin tissue or from cultured cell lines by using TRIzol (Invitrogen) or RNeasy (Qiagen), and cDNA was made from RNA by using the QuantiTect Reverse Transcription System Kit (Qiagen) or Cells-to-CT Kit (Invitrogen) according to the manufacturer's instructions. Quantitative PCR (qPCR) for hedgehog pathway genes and hypoxanthine phosphoribosyltransferase (HPRT; Applied Biosystems) was carried out by using TaqMan gene expression assays (Applied Biosystems) and species-specific primer-probe sets according to the manufacturer's specifications. Modulation of hedgehog target and pathway gene expression was determined by using the $2^{-\Delta\Delta C_t}$ method normalizing expression to that of human or mouse HPRT1.

Pharmacokinetics and pharmacodynamic effects of MEDI-5304

Female NCr nude (athymic) mice were injected subcutaneously in the right flank with 4×10^6 Colo205 cells. When the tumors reached an average of approximately 400 mm^3, the mice were randomized into control and treatment groups by stratified sampling ($n = 5$ animals/group). Control groups received a single intraperitoneal (i.p.) injection of 0.9% sodium chloride. Treatment groups were given a single intraperitoneal injection of MEDI-5304 diluted in 0.9% sodium chloride. The animals were humanely euthanized and samples were collected at various times after dose administration. Whole blood was collected by cardiac puncture. Serum was prepared and frozen at −20°C for pharmacokinetic analysis. The tumor from each animal was resected, cut into small pieces, and stored in RNA stabilization buffer for pharmacodynamic analysis.

Determination of serum MEDI-504 levels in mouse and rat

Concentrations of MEDI-5304 in mouse and rat serum were determined by using a qualified ELISA method. ELISA plates were coated with 500 ng of goat anti-human IgG (Fc specific; Thermo Scientific; cat #31125) in PBS overnight at 4°C and blocked with I-Block buffer (Tropix) for 1 hour at room temperature. MEDI-5304 reference standard, quality control, and test sample dilutions were prepared in 10% mouse or rat serum (assay matrix) and added to blocked plates for 2 hours at room temperature. Washed plates were incubated with diluted (1:20,000) secondary horseradish peroxidase (HRP)-goat anti-human IgG (Fc-specific; Thermo Scientific; cat #31413) for 1 hour at room temperature. 3,3′,5,5′-tetramethylbenzidine (TMB) substrate was incubated for 5 minutes and color development was stopped with 2 mol/L H_2SO_4. Plates were read at 450 nm with a SpectraMax Plus 384 plate reader (Molecular Devices). Concentrations of MEDI-5304 in quality control and test sample dilutions on each plate were interpolated from the reference standard curve for that plate. The range of the assay for quantification of MEDI-5304 in 100% rat serum was 31.25 to 2,000 ng/mL.

Pancreatic tumorsphere assays

Tumorspheres assays were performed by using human pancreatic tumor cells from two patient-derived xenografts (P479 and 947). Briefly, 1,000 to 3,000 cells from P479 tumors digested and dissociated into a single-cell suspension were cultured with different treatment conditions in tumorsphere medium containing 1% N2 supplement (Invitrogen), 2% B27 supplement (Invitrogen), 1% antibiotic–antimycotic (Invitrogen), 20 ng/mL basic fibroblast growth factor-2 (bFGF-2; Invitrogen), and 20 ng/mL EGF (Invitrogen) in 6-well ultralow

attachment plates (Corning) for 4 days. All cultures were analyzed for tumorsphere formation by counting using an inverted microscope or by measuring total cell viability using CellTiter-Glo Luminescent Cell Viability Assay (Promega Biosciences, Inc.) according to the manufacturer's recommendations. Luminescence was measured by using an Envision plate reader with an integration time of 1 s/well.

In vivo efficacy experiments

Experiments performed by using the HT-29/MEF coimplantation model were conducted at AstraZeneca-R&D Boston according to the Institutional Animal Care and Use Committee (IACUC) guidelines as described in Hwang and colleagues (23).

Human Panc479 xenografts (passage 4–5) were maintained as a serially passaged xenograft model by using female Rag2 knockout mice (Taconic). Donor tumors were excised, cut into fragments, and placed into the right flank of each mouse with 11G trochars. MEDI-5304 diluted in PBS or gemcitabine (Gemzar; Eli Lilly) diluted in 0.9% saline were administered by an intraperitoneal injection twice per week according to the body weight (10 mL/kg) into mice once mean tumor volume had reached approximately 130 mm^3. Tumors were harvested 24 hours after last dose, weighed, and preserved in CryoStor (BioLife Solutions) on ice before being stored at −80°C until CSC analysis. Tumor volumes and body weight measurements were recorded twice a week.

Experiments performed by orthotopic implantation of primary pancreatic explant models 890 and 947 were carried out by using 8-week-old male NOD/SCID mice that were anesthetized using an intraperitoneal injection of 100 mg/kg ketamine and 5 mg/kg xylazine. Single-cell suspensions of patient-derived pancreatic cancer cells were made with serum-free RPMI/Matrigel (BD Bioscience) mixture (1:1 volume), infected with luciferase-expressing retrovirus and 5×10^5 cells injected into the pancreatic tail as previously described (22). Animals were either untreated or treated with MEDI-5304 and gemcitabine (Gemzar; Eli Lilly), either alone or in some cases in combination, administered by intraperitoneal injection at the indicated dose levels twice per week according to the body weight (10 mL/kg). Tumor measurements of orthotopically implanted tumors were performed weekly by using bioluminescent imaging. After 4 weeks of treatment, some tumors were harvested 24 hours after last dose and digested for CSC analysis as described previously (22). General health of mice was monitored daily and all studies done at MedImmune and the University of Michigan (Ann Arbor, MI) were performed in accordance with IACUC guidelines.

Additional experimental protocols describing the exploratory rat and cynomolgus monkey toxicology studies including pharmacokinetic and pharmacodynamic analyses are provided in the Supplementary Materials and Methods.

Results

Isolation of hedgehog antibodies and characterization of their binding properties

XenoMice (24) were immunized with recombinant protein corresponding to the N-terminal signaling domain of SHH (R&D Systems) or Chinese hamster ovary cells transiently transfected with full-length hSHH cDNA to generate specific neutralizing mAbs. Hybridomas producing antibodies capable of binding SHH were identified by using an ELISA measuring antibody binding to immobilized SHH and binding to native hSHH on the surface of 293T cells transfected with full-length hSHH cDNA. Of note, 808 hits were identified and advanced into NIH3T3-Gli reporter assays. Forty hybridomas were chosen from this group for further scale-up and analysis, of which 16 were successfully cloned and sequenced, representing 12 independent lineages.

We identified two lead antibodies, 6D7 and 3H8, that differed in their binding specificity to mammalian hedgehog proteins. 6D7 bound both SHH and IHH in ELISAs, whereas 3H8 bound only SHH (Fig. 1). Neither antibody bound DHH. Binding kinetics for the antibodies was determined by using SPR. 6D7 bound human and mouse SHH, which differ by only one amino acid, with low picomolar affinities (Table 1 and Supplementary Fig.

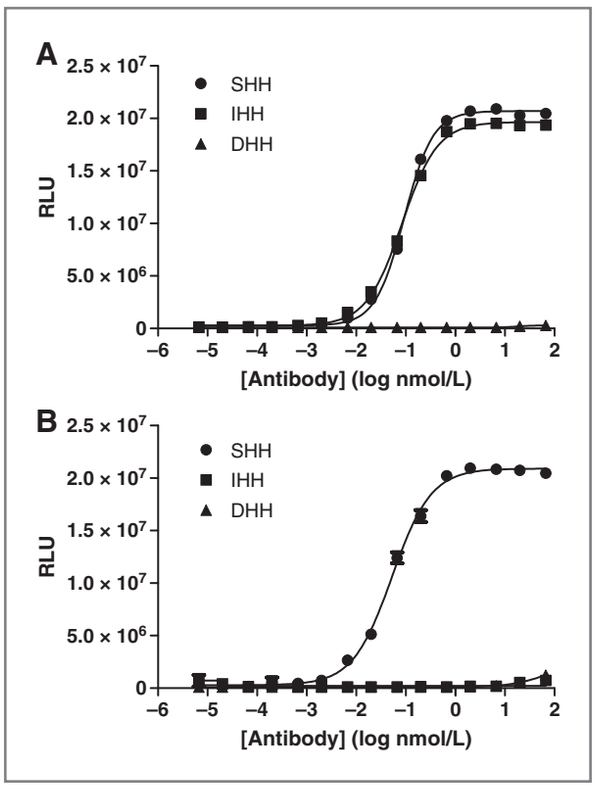

Figure 1. Differential binding of human anti-hedgehog antibodies to recombinant human hedgehog proteins. mAbs 6D7 (A) and 3H8 (B) were serially diluted and binding to recombinant human SHH C24II, IHH C28II, and DHH C23II was detected after 16 hours of incubation.

Table 1. Binding properties of anti-hedgehog antibodies

	Interaction	k_{on}, $(mol/L)^{-1}$ s^{-1}; $\times 10^7$	k_{off}, s^{-1}; $\times 10^{-4}$	K_D (k_{off}/k_{on}), pmol/L
6D7 IgG1	Human SHH	2.21 ± 0.85	1.11 ± 0.36	5.13 ± 1.04
	Mouse SHH	2.39 ± 0.46	2.92 ± 0.45	12.6 ± 4.31
	Human/mouse IHH	3.15 ± 0.90	10.9 ± 2.93	34.7 ± 0.07
3H8 IgG1	Human SHH	0.24 ± 0.08	0.83 ± 0.09	35.90 ± 7.59
	Mouse SHH	0.20 ± 0.07	1.45 ± 0.03	78.2 ± 30.6
	Human/mouse IHH	No binding	No binding	No binding
5E1 mIgG1	Human SHH	14.2 ± 3.0[a]	182 ± 16	130.8 ± 17.3
	Human/mouse IHH	6.21 ± 0.76[a]	103 ± 13	159 ± 10

NOTE: The binding kinetics of hedgehog antibodies to human and mouse SHH and IHH hedgehog proteins were determined using SPR. SPR-derived kinetic (k_{on}, k_{off}) and equilibrium dissociation constants (K_D) for the binding of recombinant human and mouse SHH and IHH to 6D7 and 3H8 human IgG1 and 5E1 mouse IgG1 antibodies are shown. Values represent mean ± SD from two or three independent experiments and were uniquely determined by the Biaevaluation software.

[a]The rates of SHH and IHH association with 5E1 are at the limit of detection for the Biacore instrument and are likely mass transport limited.

S1), but it displayed reduced affinity for IHH. The affinities of 3H8 for human and mouse SHH were 6- to 7-fold lower than the affinities observed for 6D7. The differences in the binding specificity of 6D7 and 3H8 suggest that they could have differential biologic activity depending on the expression pattern of hedgehog ligands in a given biologic system. The profile and affinity of 6D7 and 3H8 binding to hedgehog proteins also differ from those seen with 5E1. Both novel antibodies bind SHH with higher affinity than 5E1, and 6D7 displays higher affinity binding to IHH than 5E1 (Table 1). 5E1 is reported to bind DHH, albeit with lower affinity (25), whereas neither 6D7 nor 3H8 interact with DHH.

Anti-hedgehog antibodies block mGLI1 reporter activation and inhibit osteogenesis of mouse C3H10T1/2 cells

We examined the effect of the antibodies on hedgehog signaling and function. Hedgehog ligands activate a programmed transcriptional response controlled by the transcription factor GLI1 (26). Stimulation of mouse mesenchymal cells expressing a functional SMO signaling cascade with hedgehog ligands results in the activation of a GLI1 reporter. Recombinant SHH or IHH stimulated the mGLI1 luciferase reporter in stable NIH 3T3 cells in a dose-dependent manner (Supplementary Fig. S2A), though SHH showed greater maximal activity than IHH. 6D7 effectively inhibited reporter activation by either SHH or IHH, as did 5E1, whereas 3H8 interfered with only SHH-dependent reporter activation (Fig. 2A and B).

Although numerous tumor cell lines express SHH and IHH, they typically do not respond to autocrine or paracrine ligand stimulation in culture because of inactivation of functional SMO signaling (8, 27), though the mechanism by which this occurs is unknown. Some cell lines do retain the ability to respond to exogenous hedgehog ligands, including mesenchymal C3H10T1/2 cells that differentiate into osteoblasts and express the osteogenesis marker alkaline phosphatase when treated with SHH or IHH (28, 29). SHH consistently displayed greater osteogenic activity than IHH (Supplementary Fig. S2B). 6D7 inhibited induction of osteoblast differentiation of C3H10T1/2 cells by either SHH or IHH in a dose-dependent manner, yet 3H8 blocked differentiation due to SHH but not IHH (Fig. 2C and D). Transcriptional targets of hedgehog signaling are elevated coincidently with the phenotypic effects in target cells stimulated with exogenous hedgehog ligands (28, 29). SHH and IHH induce dramatic increases in GLI1 and PTC1 RNA levels in C3H10T1/2 cells that occur in a time-dependent manner over 72 hours (not shown), though the cells were more responsive to SHH treatment and the effects on GLI1 levels by either ligand were larger than for PTC1. The neutralizing effects of 6D7 and 3H8 on ligand-dependent induction of GLI1 and PTC1 RNA mirrored their phenotypic effects (Fig. 2E and F and Supplementary Fig. S3A and S3B). 5E1 exhibited similar neutralizing activity to 6D7 in C3H10T1/2 cells (Fig. 2C and D and Supplementary Fig. S3C). The potency of each of the antibodies observed in the reporter assay and C3H10T1/2 cell systems was low (IC_{50}, ~10–15 nmol/L) given their picomolar affinities for the target. However, at the high ligand concentrations (≥30 nmol/L) required to see biologic responses in these systems, the binding of the antibody is stoichiometric rather than K_D-controlled, which would explain why the potencies do not reflect affinity values determined with SPR.

We chose to focus on characterizing the preclinical antitumor efficacy of 6D7 *in vivo* in models of paracrine hedgehog signaling and CSC self-renewal because of its higher affinity and broader selectivity profile. 6D7 was renamed MEDI-5304 and is referenced as such henceforth.

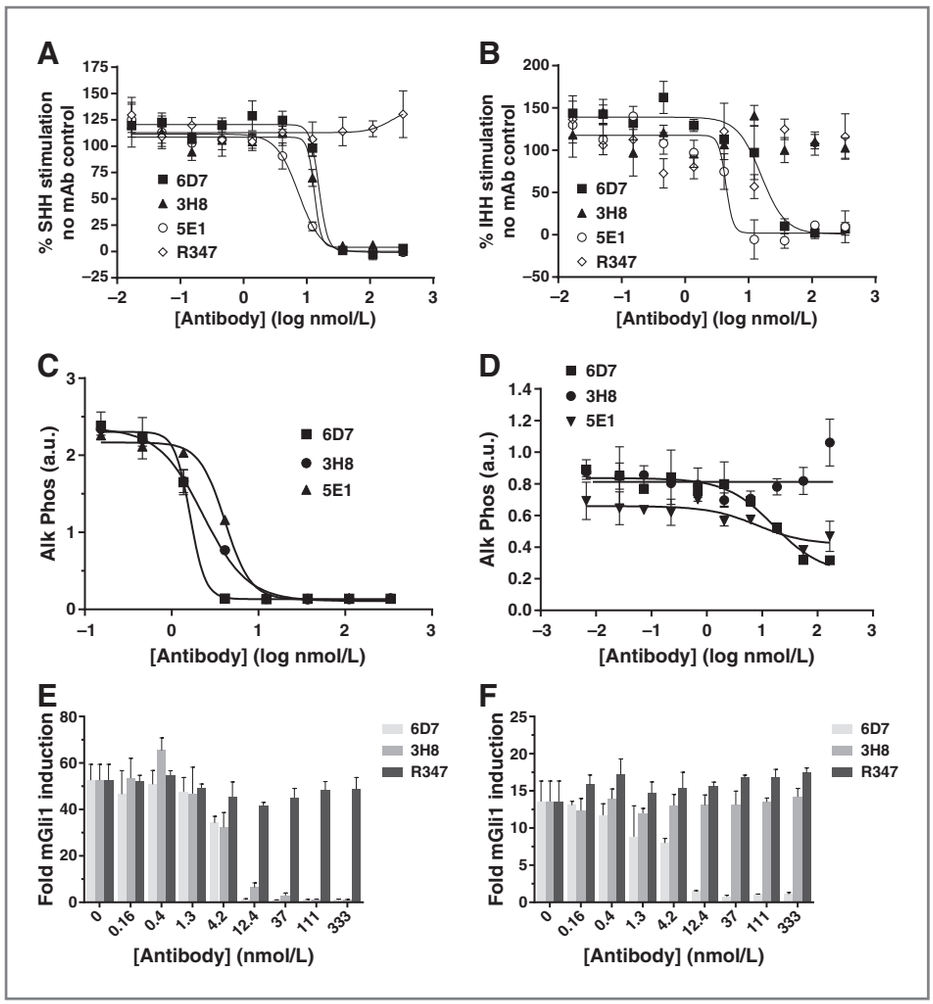

Figure 2. Neutralizing activity of anti-hedgehog mAbs in cellular assays. A and B, hedgehog antibodies inhibit the mGLI1 luciferase reporter expressed in NIH3T3 cells. Varying concentrations of 6D7, 3H8, 5E1, or negative control mAb R347 were mixed with 1 μg/mL (A) hSHH C24II or (B) human/mouse IHH C28II and incubated with cells for 24 hours. Values plotted are percentage of ligand stimulation in the absence of antibody and they represent mean ± SEM. C and D, hedgehog antibodies inhibit osteoblast differentiation of C3H10T1/2 cells induced by hedgehog ligands. C3H10T1/2 cells were treated with 600 ng/mL SHH C24II (C) or 3 μg/mL IHH C28II (D) for 3 days in the presence of serially diluted antibody. Osteoblast differentiation was measured by alkaline phosphatase (Alk Phos) activity. Values are mean ± SEM. E and F, hedgehog antibodies inhibit induction of endogenous mGLI1 by hedgehog proteins. C3H10T1/2 cells were treated with 600 ng/mL SHH C24II (E) or 2 μg/mL IHH C28II (F) for 24 hours in the absence or presence of serially diluted antibody. Modulation of endogenous levels of mGLI1 RNA by hedgehog stimulation and anti-hedgehog antibody treatment was determined by qRT-PCR. mGLI1 fold stimulation was calculated relative to unstimulated cells in the absence of antibody. Values are mean ± SEM.

Pharmacokinetics and pharmacodynamics of MEDI-5304

It was important to determine whether MEDI-5304 demonstrates biologic activity *in vivo* and what doses and levels of circulating antibody are required for activity. Secreted human hedgehog ligands stimulate expression of hedgehog target genes in mouse stromal cells but not in the tumor cells of human tumor xenografts (8, 23, 30). We used the Colo205 colon tumor model, which expresses SHH when grown as a xenograft, to ascertain whether MEDI-5304 inhibits paracrine hedgehog signaling *in vivo*. Administration of MEDI-5304 effectively inhibited hedgehog-dependent transcription in the stroma but had no effect on GLI1 RNA levels in Colo205 tumor cells, as determined with species-specific qRT-PCR (TaqMan) primers (Supplementary Fig. S4A). The differential effect of antibody treatment on tumor and stromal GLI1 RNA levels indicates that the antibody's effects are specific. We determined the effect of varying doses of MEDI-5304 on mouse GLI1 and PTC1 RNA levels in Colo205 xenografts 24 hours after dosing. Doses of 1 mg/kg and above decreased mGLI1 levels by approximately 90% and mPTC1 levels by about 75% (Fig. 3A), but lower doses had no effect. MEDI-5304 and 5E1 exhibited similar pharmacodynamic effects at doses of 1 mg/kg and above (Supplementary Fig. S4B).

The pharmacokinetic–pharmacodynamic (PK/PD) relationship for MEDI-5304 was examined over a 14-day period following an acute 1 mg/kg bolus i.p. dose. Circulating levels of MEDI-5304 reached a maximum of nearly 8 μg/mL at 4 hours and decayed over the next several days to undetectable levels by 7 days after dose administration (Fig. 3B). Pharmacodynamic effects on mGLI1 and mPTC1 RNA emerged within 4 to 6 hours after dosing and reached a maximum effect level at 24 hours, which was maintained through at least 72 hours. By 7 days when circulating antibody was no longer detected, mGLI1 and mPTC1 RNA levels were returning to normal levels. This PK/PD experiment showed that MEDI-5304 exerts extended inhibitory effects on hedgehog signaling in xenograft tumors, and that twice weekly dosing at 1 mg/kg should be sufficient to maintain target coverage.

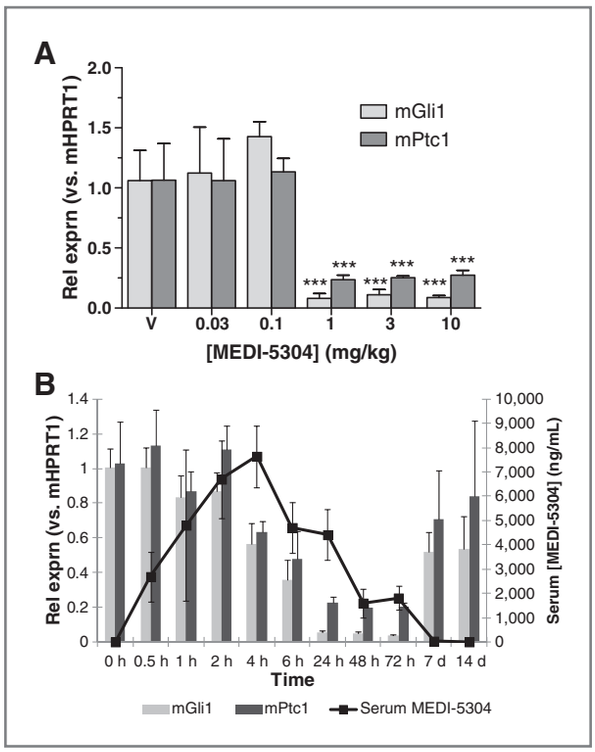

Figure 3. Pharmacokinetics and pharmacodynamics of MEDI-5304. A, MEDI-5304 displays biologic activity *in vivo*. Ncr nude mice bearing Colo205 xenograft tumors were treated intraperitoneally with vehicle or varying concentrations of antibody for 24 hours. RNA expression of mGLI1 and mPTC1 in excised tumors was determined by qRT-PCR. Values represent mean ± SEM. Statistical analysis was performed using one-way ANOVA and Dunnett multiple comparison tests, and significance (***, $P < 0.001$) is indicated when comparing antibody treatment to vehicle controls. B, PK/PD relationship of MEDI-5304 in athymic mice bearing Colo205 xenograft tumors. Athymic mice with approximately 200 mm^3 Colo205 tumors were treated with vehicle ($t = 0$) or a single 1 mg/kg i.p. dose of MEDI-5304. Tumors were excised at various times and relative mGLI1 and mPTC1 RNA levels were determined. Serum levels of MEDI-5304 were determined with a human IgG-specific ELISA.

MEDI-5304 efficacy in an *in vivo* model of paracrine hedgehog signaling

MEDI-5304 is a candidate therapeutic agent well suited to assess the importance of hedgehog function in *in vivo* efficacy models representing distinct mechanistic hypotheses because of its potency and selectivity. Yauch and colleagues (8) have argued that paracrine hedgehog signaling is the primary mechanism by which hedgehog proteins influence tumor growth. We evaluated the antitumor activity of MEDI-5304 in their *in vivo* coimplantation model by using HT-29 colon carcinoma cells and MEFs. Establishment and growth of subcutaneous HT-29 xenograft tumors are dependent on MEF coimplantation when suboptimal numbers of HT-29 cells are implanted. On the basis of PK/PD findings, we expected MEDI-3504 to have biologic activity at 1 mg/kg and above. The growth of tumors treated with doses of MEDI-5304 ≥1 mg/kg was inhibited in a statistically significant manner ($P < 0.05$; Fig. 4A), whereas the 0.1 mg/kg dose was not efficacious. 5E1 administered at 10 mg/kg displayed virtually identical antitumor activity as 10 mg/kg MEDI-5304 (Fig. 4A). All doses of MEDI-5304 and 5E1 were well tolerated. The effects of MEDI-5304 on RNA levels of several stromal hedgehog target genes were evaluated in samples collected 24 hours after the last dose. Dramatic inhibition of each target gene transcript was observed at each dose level of MEDI-5304 and 5E1 that resulted in tumor growth inhibition (Fig. 4B). The lack of effects on mGLI3 and mSMO indicated that the pharmacodynamic effects were specific for transcriptionally regulated hedgehog pathway targets.

We extended the pharmacodynamic analysis to the same set of hedgehog target genes in mouse skin samples collected during the efficacy study to understand whether MEDI-5304 activity could be detected in other tissues as a potential biomarker. Hedgehog signaling occurs in normal epidermis and modulation of hedgehog target genes by SMO antagonists in mice and human patients demonstrates that skin can be used as a surrogate tissue to assess pharmacodynamic effects of hedgehog inhibitors (31–33). Significant inhibitory effects of MEDI-5304 were limited to mGLI1 at doses of 1 mg/kg and above (Fig. 4C), which corresponds to the doses at which MEDI-5304 showed activity in xenograft tumors (Fig. 4B). Trends of dose-dependent activity were apparent for mGLI2, mPTC1, mPTC2, and mHHIP, but they did not reach statistical significance. 5E1 displayed similar pharmacodynamic effects. The explanation for the lower activity of MEDI-5304 in mouse skin than in xenograft tumors is unclear, but one possibility is that MEDI-5304 did not distribute as effectively into skin as tumors, which can be more highly vascularized. Nonetheless, significant decreases in mGLI1 suggested that the pharmacodyamics of MEDI-5304 could be assessed in skin from animals used in safety studies.

Current therapy for colon cancer includes the chemotherapeutic regimen FOLFOX [folinic acid (leucovorin), fluorouracil (5-FU), and oxaliplatin]. We evaluated whether treatment of HT-29/MEF tumors with MEDI-5304 exhibited greater efficacy in combination with carboplatin, which we used as a surrogate for the oxaliplatin component of FOLFOX. The combination of MEDI-5304 with carboplatin significantly inhibited tumor growth compared with control antibody, and the effect of combination treatment was significantly different ($P < 0.05$) than inhibition seen with MEDI-5304 or carboplatin alone (Fig. 4D). These results suggest that blockade of paracrine hedgehog signaling could improve the efficacy of chemotherapy regimen that includes platin agents in patients with colon tumors.

MEDI-5304 does not alter the prevalence of CSCs in primary pancreatic tumor explants *in vivo*

In addition to paracrine signaling, hedgehog proteins are implicated in the biology of CSCs in pancreatic adenocarcinoma. We used MEDI-5304 to investigate the

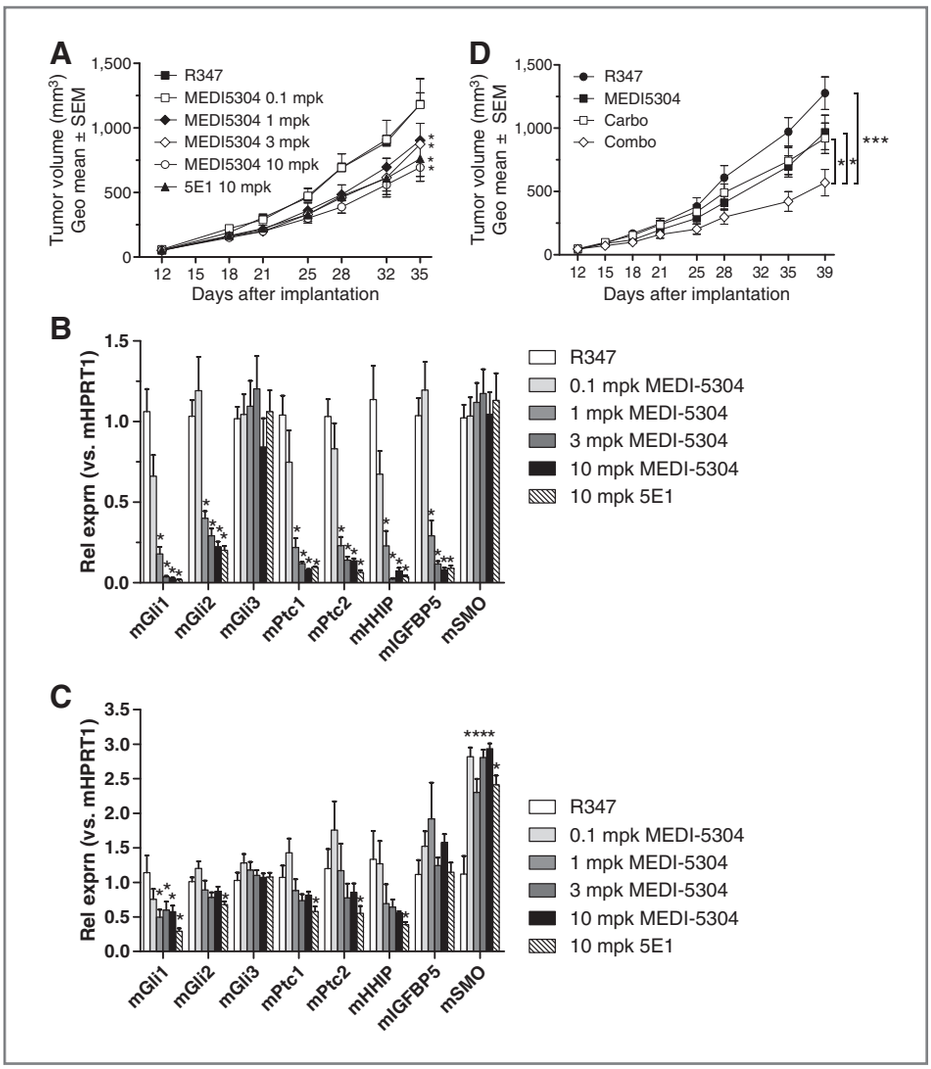

Figure 4. MEDI-5304 exhibits single agent and combination efficacy with carboplatin in a coimplant model of paracrine hedgehog signaling. A, MEDI-5304 inhibits the growth of HT-29/MEF coimplant tumors. HT-29 and MEFs were mixed (1:5 cell ratio) and implanted subcutaneously into Ncr nude mice, which were dosed (10 animals/group) intraperitoneally with varying amounts of MEDI-5304, 10 mg/kg 5E1 or 10 mg/kg R347 twice weekly starting on day 11. Tumor volumes are geometric mean ± SEM. Student *t* test was used to determine significance of MEDI-5304 or 5E1 treatment relative to R347 treatment on day 35 (*, $P < 0.05$). B and C, end of efficacy study pharmacodynamic effects of MEDI-5304 and 5E1 on hedgehog target gene expression in tumor stroma (B) and mouse skin (C). Tumors were harvested and skin samples were obtained 24 hours after last dose and RNA expression of stromal hedgehog target and pathway genes (mGLI1, mGLI2, mGLI3, mPTC1, mPTC2, mHHIP, mIGFBP-5, and mSMO) was measured using qRT-PCR. Values represent mean ± SEM. One-way ANOVA and Dunnett multiple comparison tests were used to determine statistical significance (*, $P < 0.05$) of antibody treatment compared with the R347 control group. D, MEDI-5304 enhances tumor growth inhibition of carboplatin treatment of the HT-29/MEF coimplant model. Mice with HT-29/MEF coimplant tumors received MEDI-5304 (10 mg/kg twice/week i.p.), carboplatin (30 mg/kg once/week i.p.), or both agents in combination for 4 weeks starting on day 12. Tumor volumes are geometric mean ± SEM. Student *t* test was used to determine statistical significance of combination treatment compared with R347 (***, $P < 0.001$) and significance of combination treatment compared with each agent alone (*, $P < 0.05$).

hedgehog dependence of pancreatic CSCs by assessing its effects *in vivo* on tumor growth and CSC numbers of three primary pancreatic explant models implanted either subcutaneously (P479) or orthotopically (890 and 947). The CSCs from each model expressed elevated SHH RNA (Supplementary Fig. S5A), as seen previously (22). Each model exhibited sensitivity to gemcitabine (Fig. 5A), a chemotherapeutic agent commonly used to treat patients with pancreatic cancer, but MEDI-5304 did not display single-agent activity or enhance the activity of gemcitabine in any of the models (Fig. 5A). Gemcitabine increased the CSC population in each model (Fig. 5B), as has been reported previously (34, 35), yet MEDI-5304 had no effect on CSC frequency and did not enhance the effect of gemcitabine on CSC numbers for any of the tumors studied (Fig. 5B). Biologic activity of MEDI-5304 in each model was confirmed, as it decreased stromal mGLI1 levels by >90% (data not shown).

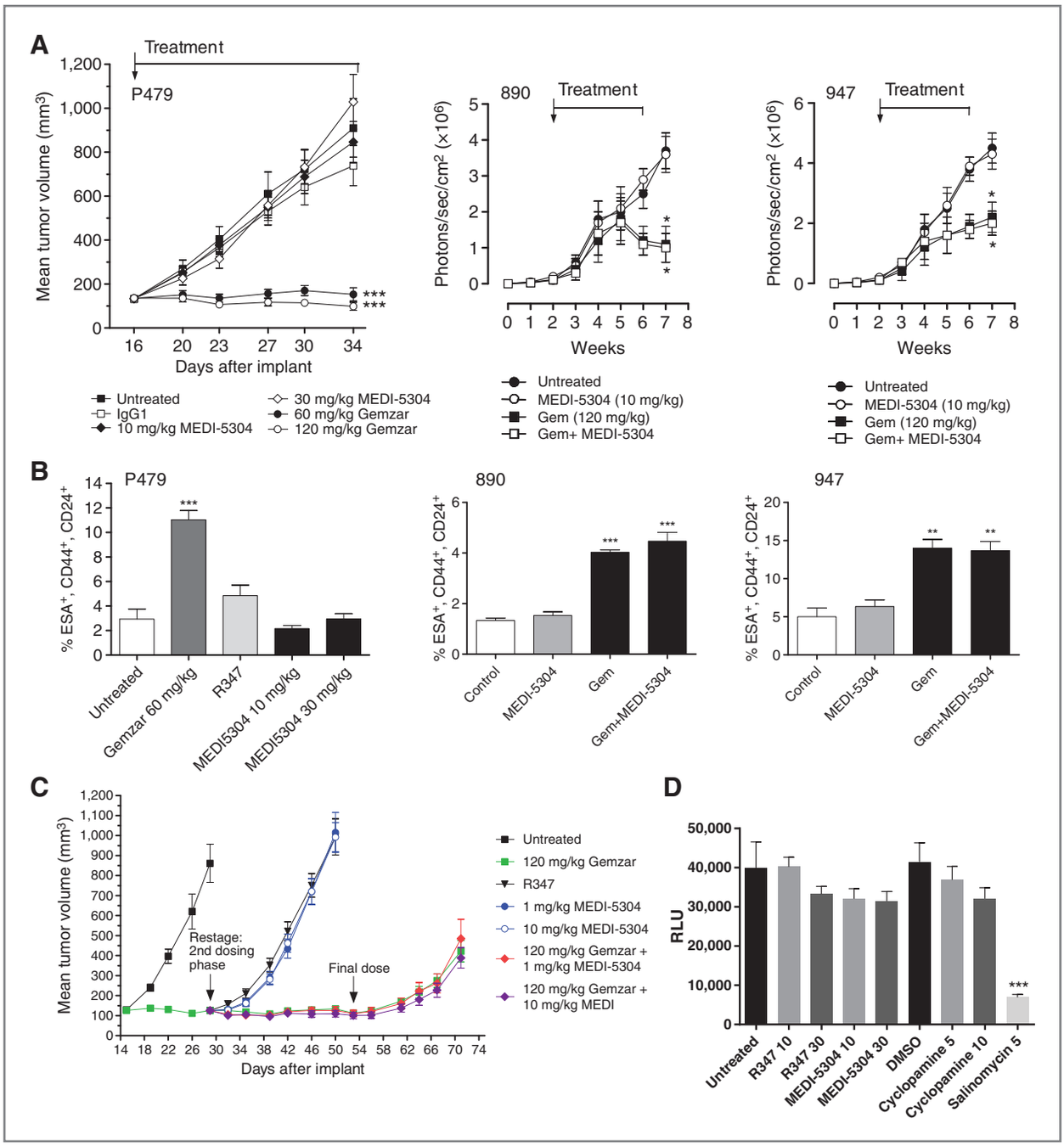

Figure 5. MEDI-5304 lacks effects on tumor growth and CSCs in primary pancreatic explants models. A, MEDI-5304 lacks antitumor activity against three primary pancreatic explant models. RAG2 knockout mice (10 mice/group) with subcutaneous P479 tumors were treated with R347 (10 mg/kg), MEDI-5304 (10 or 30 mg/kg), or gemcitabine (60 or 120 mg/kg) given intraperitoneally twice a week starting on day 16. Animals with orthotopic tumors from models 890 and 947 (8 mice/group) were untreated or received MEDI-5304 (10 mg/kg), gemcitabine (120 mg/kg), or both treatments in combination. Student *t* test was used to determine significance of each treatment compared with the untreated control (*, $P < 0.05$; ***, $P < 0.001$). B, MEDI-5304 has no effect on CSC frequency in primary pancreatic tumor models. End of study samples were collected 24 hours after last dose on a minimum of three samples per treatment arm and flow cytometry analysis of the CSC population (ESA^+, $CD44^+$, and $CD24^+$) was performed. Data are presented as % CSC, the percentage of cells staining positive for all three markers. Statistical analysis was performed using one-way ANOVA and Dunnett multiple comparison tests (**, $P < 0.01$; ***, $P < 0.001$). C, MEDI-5304 does not improve responsiveness to gemcitabine pretreatment or coadministration. Mice with subcutaneous P479 tumors were either untreated (closed black squares) or treated intraperitoneally with 120 mg/kg gemcitabine every 4 days for four doses (closed green squares). (*Continued on the following page*.)

We evaluated whether use of MEDI-5304 in a maintenance setting would improve responses to gemcitabine by impairing CSCs. We treated P479 tumors with gemcitabine to enrich for CSCs and subsequently administered MEDI-5304 alone or in combination with gemcitabine. Administration of MEDI-5304 following gemcitabine treatment resulted in rapid tumor regrowth, and addition of MEDI-5304 to gemcitabine did not improve responses (Fig. 5C). Gemcitabine-containing treatment arms were discontinued on day 53 to allow tumor outgrowth, but prior MEDI-5304 treatment had no inhibitory effect on regrowth. Finally, MEDI-5304 lacked activity in tumorsphere assays by using dissociated cells from two different patient tumors, whereas the anti-CSC compound salinomycin (36) blocked tumorsphere formation (Fig. 5D and Supplementary Fig. S5B). These results indicate that MEDI-5304 lacked activity against pancreatic CSCs *in vitro* and *in vivo* and was unable to affect corresponding tumorsphere or tumor growth of these models, supporting the conclusion that hedgehog function is not essential for pancreatic CSC maintenance or self-renewal.

Exploratory toxicology in rats and cynomolgus monkeys

We performed a 2-week pilot toxicity study with MEDI-5304 in rats during which animals received vehicle, 10 or 50 mg/kg MEDI-5304 on day 0 and 7, and the subjects were subsequently necropsied on day 14. Doses were chosen on the basis of a preliminary single dose rat pharmacokinetic study, which indicated a trend of an antigen sink that is saturated at MEDI-5304 doses of greater than 10 mg/kg (Supplementary Fig. S6). MEDI-5304 did not affect appearance, behavior, body weights, hematology, coagulation, or clinical chemistry parameters. Microscopic evaluation of tissues showed that the only drug-related finding was odontodysplasia noted in the incisor teeth in the 50 mg/kg group. The change was characterized by loss of odontoblast cell layer polarity accompanied by deposits of dentin-like material (Supplementary Fig. S7), a finding consistent with disruption of SHH function in the tooth germ (37).

In addition, a nonterminal safety study was conducted in cynomolgus monkeys to evaluate PK/PD and toxicity of MEDI-5304. Animals received either PBS or MEDI-5304 intravenously at an initial single low dose of either 0.3, 1, or 3 mg/kg followed 2 weeks later by escalated doses of 3, 10, or 75 mg/kg antibody every week $\times$ 3 weeks. MEDI-5304 levels in serum were within the expected range for a human IgG in cynomolgus monkey, with a trend toward an antigen sink saturated at 1 mg/kg (Supplementary Fig. S8). There were no changes in clinical signs, body weights, or clinical pathology parameters, including Troponin I, Troponin T, or creatine kinase isozymes. However, pharmacodynamic effects were observed in skin punch biopsies taken on day 4. GLI1, PTCH1, and PTCH2 RNA levels were decreased (Supplementary Fig. S9) at all doses, similar to observations in mouse skin samples (Fig. 4C). The results of the preclinical rat and cynomolgus toxicology studies support the preliminary conclusion that MEDI-5304 likely has a sufficient safety margin to allow testing the clinical hypothesis that neutralizing hedgehog function with MEDI-5304 in tumors with elevated SHH or IHH will be efficacious.

Discussion

We describe here the isolation of two novel neutralizing hedgehog mAbs with differential selectivity for the three mammalian isoforms of hedgehog. 6D7 (MEDI-5304) binds SHH and IHH with high affinity and inhibits their activity in cellular reporter assays and functional assays of osteoblast differentiation. 3H8 is selective for SHH, inhibiting its activity in reporter and osteogenesis assays, but it exhibits slightly lower binding affinity than 6D7. MEDI-5304 (6D7) is biologically active *in vivo*, demonstrating pharmacodynamic effects on hedgehog signaling in stromal cells at doses as low as 1 mg/kg. MEDI-5304 displayed antitumor activity in the HT-29/MEF coimplantation model when administered as a single agent and in combination with carboplatin. MEDI-5304 exhibited higher affinity binding to SHH and IHH than mouse mAb 5E1, but MEDI-5304 and 5E1 displayed similar activity in cellular mechanistic and phenotypic assays and in *in vivo* pharmacodynamic and efficacy studies. These findings may be explained by preliminary competition binding studies indicating that MEDI-5304 and 5E1 do not cross-compete for binding to SHH and as such bind different epitopes (data not shown). Finally, the only signal attributed to MEDI-5304 in preclinical rat and cynomolgus primate safety studies was mechanism-based odontodysplasia of rat incisors at the 50 mg/kg dose. These findings indicate that MEDI-5304 represents an attractive candidate to continue clinical development in patients with tumors resulting from elevated SHH or IHH.

(*Continued*.) Animals receiving gemcitabine were then re-randomized on day 29 into groups of 10 mice/group, which then received one of the following treatment regimen every 4 days: 10 mg/kg R347 (closed black triangles), 120 mg/kg gemcitabine (closed green squares), 1 mg/kg MEDI-5304 (closed blue circles), 10 mg/kg MEDI-5304 (open blue circles), combination of 120 mg/kg gemcitabine and 1 mg/kg MEDI-5304 (closed red diamonds), or combination of 120 mg/kg gemcitabine and 10 mg/kg MEDI-5304 (closed purple diamonds). Tumors in mice that did not receive gemcitabine during the second dosing phase grew to approximately 1,000 mm^3 and these mice were sacrificed on day 50. The second phase of dosing for animals that received gemcitabine as part of the dosing regimen was discontinued on day 53, and outgrowth of those tumors was monitored until day 71. No differences among these three groups were detected. D, MEDI-5304 does not affect P479 tumorpshere growth. Dissociated cells from P479 tumors were plated in media that promotes tumorsphere formation. Cells were plated in the absence or presence of 10 or 30 μg/mL negative control antibody R347, 10 or 30 μg/mL MEDI-5304, 5 or 10 μmol/L cyclopamine, or salinomycin (2 μmol/L). Statistical analysis was performed using one-way ANOVA and Dunnett multiple comparison tests. Statistical significance (***, $P < 0.001$) is indicated for salinomycin in comparison with the DMSO control.

Initial observations linking the hedgehog pathway to tumorigenesis and tumor growth suggested autocrine signaling (5–7, 38). However, it has been difficult to model autocrine effects on tumor cells because the pathway seems to be inactivated shortly after initial model propagation *in vitro* and *in vivo* (27). In addition, paracrine hedgehog signaling has been described in primary patient samples. Coincident expression of SHH in tumor cells and GLI1 in the stroma has been reported in invasive breast, pancreatic, and metastatic liver tumors (8, 9, 39, 40). Recent experimental evidence supports a paracrine signaling model whereby hedgehog ligands produced by tumor cells exert biologic effects on stromal cells, which then in turn promote tumor growth and metastasis (8, 40). Potential stromal target cells include myofibroblasts and perivascular stromal cells (23, 30).

We used the potent and selective hedgehog pathway inhibitor MEDI-5304 to assess the paracrine hedgehog signaling hypothesis. Coimplantation of MEFs, myofibroblasts, or human pancreatic stellate cells (HPSC) has been used to support tumor establishment and growth of colon and pancreatic xenograft tumor models (8, 23). MEDI-5304 inhibited the growth of the HT-29/MEF coimplant model, which corresponded to pharmacodynamic effects on hedgehog target genes in the stroma but not in tumor cells. Similar results were seen with the SMO inhibitor AZD8542 (23). MEDI-5304 had no effect on the growth of HT-29 xenografts implanted without MEFs (data not shown). Similarly, BxPC3 pancreatic xenograft tumor growth was sensitive to disruption of HH/SMO signaling due to AZD8542 treatment, but only when coimplanted with HPSCs (23). Thus, the antitumor activity of MEDI-5304 in the HT-29/MEF coimplant model supports the hypothesis that paracrine hedgehog signaling can promote tumor formation and growth.

Hedgehog function is implicated in CSC biology (21). SHH and IHH RNA expression is elevated in CSCs of multiple primary pancreatic tumor explant models [(22) and Supplementary Fig. S5A]. Pancreatic tumorspheres, which are enriched in cells with stem cell–like properties, have increased levels of hedgehog pathways components (41). Treatment of cell lines and tumorspheres *in vitro* with SMO antagonists cyclopamine and IPI-926 reduced the number of CSCs defined as $ALDH^+$ or $CD133^+$, and cyclopamine inhibited Panc-1 tumorsphere growth (16, 41–43). However, the anti-proliferative and apoptotic effects of cyclopamine and related compounds may be off-target as they are observed broadly in tumor cells in which active ligand-dependent hedgehog signaling is not evident. These effects may be the result of neutral sphingomyelin phosphodiesterase 3 (nSMase2) activity and ceramide production rather than inhibition of hedgehog signaling (44). These findings led us to evaluate whether hedgehog signaling is required for CSC self-renewal or maintenance in primary pancreatic cancer explant models using the highly selective and potent antibody MEDI-5304. MEDI-5304 had no effect on tumorspheres from two independent primary models, and it did not alter CSC frequency or inhibit tumor growth of three primary pancreatic cancer xenograft models when used as a single agent, indicating that ligand-dependent hedgehog pathway activity does not regulate CSCs numbers in primary models of pancreatic cancer.

CSCs are often insensitive to chemotherapeutic agents, resulting in accumulation of CSCs following treatment with such agents (21). Gemcitabine treatment of primary pancreatic models results in CSC enrichment (34, 35), and gemcitabine-resistant pancreatic cells express elevated levels of pancreatic CSC markers (45, 46). This evidence suggests simultaneous or sequential combination treatment with chemotherapy and agents that kill CSCs will lead to more effective antitumor responses and prevent development of resistance, as has been reported for combination treatment of primary colon xenografts with DLL4 antibodies and irinotecan (47). It has been argued that blocking hedgehog signaling with cyclopamine sensitizes pancreatic CSCs to chemotherapy (41, 46). For example, treatment of primary pancreatic model Panc185 with gemcitabine alone resulted in tumor stasis, whereas administration of cyclopamine and gemcitabine caused tumor regression (48). Because of the concerns that cyclopamine can act on pathways other than the hedgehog pathway, we asked whether treating primary pancreatic tumor models with gemcitabine to kill differentiated cells but spare CSCs in combination with the specific neutralizing antibody MEDI-5304 would lead to synergistic responses *in vivo*.

We observed that gemcitabine treatment caused accumulation of CSCs in the three pancreatic models we evaluated, which coincided with tumor growth inhibition (Fig 5A and B). However, addition of MEDI-5304 to gemcitabine therapy did not modulate its effects on CSC prevalence or tumor growth *in vivo*. Furthermore, exploration of sequential and combination dosing of gemcitabine and MEDI-5304 in the P479 model indicated that MEDI-5304 did not improve responses to gemcitabine under conditions where gemcitabine treatment would have enriched for CSCs and presumably rendered tumors more dependent on this cell population for growth (Fig. 5C). These results indicate that the hedgehog pathway is not essential for CSC function in pancreatic cancer. However, pancreatic CSC populations defined by markers other than ESA/CD44/CD24 may differentially depend on hedgehog function. Our results also do not preclude the possibility that MEDI-5304 may inhibit tumor growth, metastasis, or development of resistance by impairing CSCs in other tumor types. Nonetheless, our findings support the paracrine hedgehog signaling hypothesis, suggesting that tumors that depend on paracrine hedgehog signaling between tumor cells expressing hedgehog ligands and responsive stromal cells are most likely to respond to MEDI-5304.

Several SMO antagonists have advanced to clinical trials and the first of those agents, vismodegib, has been approved for the treatment of locally advanced and metastatic BCC (18, 49). Vismodegib has also displayed

clinical activity in medulloblasoma (19). The clinical activity of vismodegib in these indications is observed in patients with tumors harboring mutations in *PTCH* or *SMO* that constitutively activate the pathway. However, results from phase II clinical trials with vismodegib or saridegib in disease indications where overexpression of hedgehog ligands rather than mutational activation of the pathway is observed have been less encouraging (49). These outcomes suggest that alternative approaches to inhibiting hedgehog signaling, such as neutralizing hedgehog antibodies, may be required for improved responses in these settings.

In summary, we describe high-affinity fully human antibodies to SHH and IHH that demonstrated neutralizing activity *in vitro* and *in vivo*. The dual hedgehog inhibitor MEDI-5304 exhibited robust pharmacodynamic effects and antitumor activity in a xenograft model of paracrine hedgehog signaling. As such, MEDI-5304 is an attractive clinical candidate for the treatment of hedgehog pathway-dependent tumors resulting from elevated hedgehog proteins.

Disclosure of Potential Conflicts of Interest

N. Laing has ownership interest in stock and patent. M. Liang has ownership interest in AstraZeneca stocks. D.M. Simeone has a commercial research grant from MedImmune. D.C. Blakey has ownership interest in AstraZeneca. No potential conflicts of interest were disclosed by the other authors.

Authors' Contributions

Conception and design: N.R. Michaud, Y. Wang, J.S. Kang, N. Laing, D.W. Jenkins, E. Hurt, M. Liang, C. Frantz, R.E. Hollingsworth, D.C. Blakey, V. Bedian

Development of methodology: K. McEachern, A. Hernandez, J. Jovanović, E. Hurt, M. Liang, C. Frantz

Acquisition of data (provided animals, acquired and managed patients, provided facilities, etc.): Y. Wang, K. McEachern, J.J. Jordan, A.M. Mazzola, S. Jalla, J.W. Chesebrough, M.J. Hynes, M. Belmonte, L. Wang, J.S. Kang, J. Jovanović, E. Hurt, M. Liang, C. Frantz, D.M. Simeone

Analysis and interpretation of data (e.g., statistical analysis, biostatistics, computational analysis): N.R. Michaud, Y. Wang, K. McEachern, J.J. Jordan, A.M. Mazzola, A. Hernandez, S. Jalla, M. Belmonte, J.S. Kang, J. Jovanović, N. Laing, D.W. Jenkins, E. Hurt, M. Liang, C. Frantz, R.E. Hollingsworth, D.M. Simeone

Writing, review, and/or revision of the manuscript: N.R. Michaud, Y. Wang, K. McEachern, A.M. Mazzola, S. Jalla, J.W. Chesebrough, J. Jovanović, N. Laing, D.W. Jenkins, E. Hurt, M. Liang, C. Frantz, R.E. Hollingsworth, D.M. Simeone, D.C. Blakey, V. Bedian

Administrative, technical, or material support (i.e., reporting or organizing data, constructing databases): J.J. Jordan, A.M. Mazzola, J.W. Chesebrough, M. Liang, C. Frantz

Study supervision: N.R. Michaud, Y. Wang, D.W. Jenkins, M. Liang, C. Frantz, R.E. Hollingsworth, V. Bedian

Acknowledgments

The authors thank Christine Pien, Shenghua Wen, Hong Lu, Ling Du, Ling Fu, Patrick Strout, Zach Brohawn, and Ying Li for technical assistance. The authors also thank Jin Gao, Yong Chang, and Alex Cao for productive discussions during the course of this work, and Stephen Scott, Lily Cheng, and Mark Mense for contributions to the toxicology studies.

Grant Support

This work was funded by AstraZeneca PLC and MedImmune LLC.

The costs of publication of this article were defrayed in part by the payment of page charges. This article must therefore be hereby marked *advertisement* in accordance with 18 U.S.C. Section 1734 solely to indicate this fact.

Received May 24, 2013; revised November 27, 2013; accepted December 11, 2013; published OnlineFirst December 15, 2013.

References

1. Borzillo GV, Lippa B. The hedgehog signaling pathway as a target for anticancer drug discovery. Curr Top Med Chem 2005;5:147–57.
2. Varjosalo M, Taipale J. Hedgehog: functions and mechanisms. Genes Dev 2008;22:2454–72.
3. Evangelista M, Tian H, de Sauvage FJ. The hedgehog signaling pathway in cancer. Clin Cancer Res 2006;12:5924–8.
4. Teglund S, Toftgard R. Hedgehog beyond medulloblastoma and basal cell carcinoma. Biochim Biophys Acta 2010;1805:181–208.
5. Kar S, Deb M, Sengupta D, Shilpi A, Bhutia SK, Patra SK. Intricacies of hedgehog signaling pathways: a perspective in tumorigenesis. Exp Cell Res 2012;318:1959–72.
6. Berman DM, Karhadkar SS, Maitra A, Montes De Oca R, Gerstenblith MR, Briggs K, et al. Widespread requirement for hedgehog ligand stimulation in growth of digestive tract tumours. Nature 2003;425:846–51.
7. Karhadkar SS, Bova GS, Abdallah N, Dhara S, Gardner D, Maitra A, et al. Hedgehog signalling in prostate regeneration, neoplasia and metastasis. Nature 2004;431:707–12.
8. Yauch RL, Gould SE, Scales SJ, Tang T, Tian H, Ahn CP, et al. A paracrine requirement for hedgehog signalling in cancer. Nature 2008;455:406–10.
9. O'Toole SA, Machalek DA, Shearer RF, Millar EK, Nair R, Schofield P, et al. Hedgehog overexpression is associated with stromal interactions and predicts for poor outcome in breast cancer. Cancer Res 2011;71:4002–14.
10. Watkins DN, Berman DM, Burkholder SG, Wang B, Beachy PA, Baylin SB. Hedgehog signalling within airway epithelial progenitors and in small-cell lung cancer. Nature 2003;422:313–7.
11. Thayer SP, di Magliano MP, Heiser PW, Nielsen CM, Roberts DJ, Lauwers GY, et al. Hedgehog is an early and late mediator of pancreatic cancer tumorigenesis. Nature 2003;425:851–6.
12. Oro AE, Higgins KM, Hu Z, Bonifas JM, Epstein EH Jr, Scott MP. Basal cell carcinomas in mice overexpressing sonic hedgehog. Science 1997;276:817–21.
13. Lee MJ, Hatton BA, Villavicencio EH, Khanna PC, Friedman SD, Ditzler S, et al. Hedgehog pathway inhibitor saridegib (IPI-926) increases lifespan in a mouse medulloblastoma model. Proc Natl Acad Sci U S A 2012;109:7859–64.
14. Olive KP, Jacobetz MA, Davidson CJ, Gopinathan A, McIntyre D, Honess D, et al. Inhibition of hedgehog signaling enhances delivery of chemotherapy in a mouse model of pancreatic cancer. Science 2009;324:1457–61.
15. McCann CK, Growdon WB, Kulkarni-Datar K, Curley MD, Friel AM, Proctor JL, et al. Inhibition of hedgehog signaling antagonizes serous ovarian cancer growth in a primary xenograft model. PLoS ONE 2011;6:e28077.
16. Feldmann G, Fendrich V, McGovern K, Bedja D, Bisht S, Alvarez H, et al. An orally bioavailable small-molecule inhibitor of hedgehog signaling inhibits tumor initiation and metastasis in pancreatic cancer. Mol Cancer Ther 2008;7:2725–35.
17. Romer JT, Kimura H, Magdaleno S, Sasai K, Fuller C, Baines H, et al. Suppression of the shh pathway using a small molecule inhibitor eliminates medulloblastoma in Ptc1(+/−)p53(−/−) mice. Cancer Cell 2004;6:229–40.
18. Sekulic A, Migden MR, Oro AE, Dirix L, Lewis KD, Hainsworth JD, et al. Efficacy and safety of vismodegib in advanced basal-cell carcinoma. N Engl J Med 2012;366:2171–9.

19. Rudin CM, Hann CL, Laterra J, Yauch RL, Callahan CA, Fu L, et al. Treatment of medulloblastoma with hedgehog pathway inhibitor GDC-0449. N Engl J Med 2009;361:1173–8.
20. Beachy PA, Hymowitz SG, Lazarus RA, Leahy DJ, Siebold C. Interactions between Hedgehog proteins and their binding partners come into view. Genes Dev 2010;24:2001–12.
21. Zhou BB, Zhang H, Damelin M, Geles KG, Grindley JC, Dirks PB. Tumour-initiating cells: challenges and opportunities for anticancer drug discovery. Nat Rev Drug Discov 2009;8:806–23.
22. Li C, Heidt DG, Dalerba P, Burant CF, Zhang L, Adsay V, et al. Identification of pancreatic cancer stem cells. Cancer Res 2007; 67:1030–7.
23. Hwang RF, Moore TT, Hattersley MM, Scarpitti M, Yang B, Devereaux E, et al. Inhibition of the hedgehog pathway targets the tumor-associated stroma in pancreatic cancer. Mol Cancer Res 2012; 10:1147–57.
24. Green LL. Antibody engineering via genetic engineering of the mouse: XenoMouse strains are a vehicle for the facile generation of therapeutic human monoclonal antibodies. J Immunol Methods 1999;231:11–23.
25. Maun HR, Wen X, Lingel A, de Sauvage FJ, Lazarus RA, Scales SJ, et al. Hedgehog pathway antagonist 5E1 binds hedgehog at the pseudo-active site. J Biol Chem 2010;285:26570–80.
26. Ruiz i Altaba A, Mas C, Stecca B. The gli code: an information nexus regulating cell fate, stemness and cancer. Trends Cell Biol 2007; 17:438–47.
27. Sasai K, Romer JT, Lee Y, Finkelstein D, Fuller C, McKinnon PJ, et al. Shh pathway activity is down-regulated in cultured medulloblastoma cells: implications for preclinical studies. Cancer Res 2006;66: 4215–22.
28. Nakamura T, Aikawa T, Iwamoto-Enomoto M, Iwamoto M, Higuchi Y, Pacifici M, et al. Induction of osteogenic differentiation by hedgehog proteins. Biochem Biophys Res Commun 1997;237:465–9.
29. Williams KP, Rayhorn P, Chi-Rosso G, Garber EA, Strauch KL, Horan GS, et al. Functional antagonists of sonic hedgehog reveal the importance of the N terminus for activity. J Cell Sci 1999;112: 4405–14.
30. Chen W, Tang T, Eastham-Anderson J, Dunlap D, Alicke B, Nannini M, et al. Canonical hedgehog signaling augments tumor angiogenesis by induction of VEGF-A in stromal perivascular cells. Proc Natl Acad Sci U S A 2011;108:9589–94.
31. Ikram MS, Neill GW, Regl G, Eichberger T, Frischauf AM, Aberger F, et al. GLI2 is expressed in normal human epidermis and BCC and induces GLI1 expression by binding to its promoter. J Invest Dermatol 2004;122:1503–9.
32. Rohner A, Spilker ME, Lam JL, Pascual B, Bartkowski D, Li QJ, et al. Effective targeting of hedgehog signaling in a medulloblastoma model with PF-5274857, a potent and selective smoothened antagonist that penetrates the blood-brain barrier. Mol Cancer Ther 2012;11:57–65.
33. LoRusso PM, Rudin CM, Reddy JC, Tibes R, Weiss GJ, Borad MJ, et al. Phase I trial of hedgehog pathway inhibitor vismodegib (GDC-0449) in patients with refractory, locally advanced or metastatic solid tumors. Clin Cancer Res 2011;17:2502–11.
34. Hermann PC, Huber SL, Herrler T, Aicher A, Ellwart JW, Guba M, et al. Distinct populations of cancer stem cells determine tumor growth and metastatic activity in human pancreatic cancer. Cell Stem Cell 2007; 1:313–23.
35. Bednar F, Simeone DM. Pancreatic cancer stem cell biology and its therapeutic implications. J Gastroenterol 2011;46:1345–52.
36. Gupta PB, Onder TT, Jiang G, Tao K, Kuperwasser C, Weinberg RA, et al. Identification of selective inhibitors of cancer stem cells by high-throughput screening. Cell 2009;138:645–59.
37. Cobourne MT, Sharpe PT. Sonic hedgehog signaling and the developing tooth. Curr Top Dev Biol 2005;65:255–87.
38. Varnat F, Duquet A, Malerba M, Zbinden M, Mas C, Gervaz P, et al. Human colon cancer epithelial cells harbour active HEDGEHOG-GLI signalling that is essential for tumour growth, recurrence, metastasis and stem cell survival and expansion. EMBO Mol Med 2009;1:338–51.
39. Bailey JM, Swanson BJ, Hamada T, Eggers JP, Singh PK, Caffery T, et al. Sonic hedgehog promotes desmoplasia in pancreatic cancer. Clin Cancer Res 2008;14:5995–6004.
40. Tian H, Callahan CA, DuPree KJ, Darbonne WC, Ahn CP, Scales SJ, et al. Hedgehog signaling is restricted to the stromal compartment during pancreatic carcinogenesis. Proc Natl Acad Sci U S A 2009; 106:4254–9.
41. Huang FT, Zhuan-Sun YX, Zhuang YY, Wei SL, Tang J, Chen WB, et al. Inhibition of hedgehog signaling depresses self-renewal of pancreatic cancer stem cells and reverses chemoresistance. Int J Oncol 2012;41:1707–14.
42. Feldmann G, Dhara S, Fendrich V, Bedja D, Beaty R, Mullendore M, et al. Blockade of hedgehog signaling inhibits pancreatic cancer invasion and metastases: a new paradigm for combination therapy in solid cancers. Cancer Res 2007;67:2187–96.
43. Mueller MT, Hermann PC, Witthauer J, Rubio-Viqueira B, Leicht SF, Huber S, et al. Combined targeted treatment to eliminate tumorigenic cancer stem cells in human pancreatic cancer. Gastroenterology 2009;137:1102–13.
44. Meyers-Needham M, Lewis JA, Gencer S, Sentelle RD, Saddoughi SA, Clarke CJ, et al. Off-target function of the Sonic hedgehog inhibitor cyclopamine in mediating apoptosis via nitric oxide-dependent neutral sphingomyelinase 2/ceramide induction. Mol Cancer Ther 2012;11: 1092–1102.
45. Hong SP, Wen J, Bang S, Park S, Song SY. CD44-positive cells are responsible for gemcitabine resistance in pancreatic cancer cells. Int J Cancer 2009;125:2323–31.
46. Yao J, An Y, Wie JS, Ji ZL, Lu ZP, Wu JL, et al. Cyclopamine reverts acquired chemoresistance and down-regulates cancer stem cell markers in pancreatic cancer cell lines. Swiss Med Wkly 2011;141:w13208.
47. Hoey T, Yen WC, Axelrod F, Basi J, Donigian L, Dylla S, et al. DLL4 blockade inhibits tumor growth and reduces tumor-initiating cell frequency. Cell Stem Cell 2009;5:168–77.
48. Jimeno A, Feldmann G, Suarez-Gauthier A, Rasheed Z, Solomon A, Zou GM, et al. A direct pancreatic cancer xenograft model as a platform for cancer stem cell therapeutic development. Mol Cancer Ther 2009;8:310–4.
49. McMillan R, Matsui W. Molecular pathways: the hedgehog signaling pathway in cancer. Clin Cancer Res 2012;18:4883–8.